



Low mercury risks in paddy soils across the Pakistan

Muhammad Wajahat Aslam^a, Bo Meng^{a,*}, Waqar Ali^b, Muhammad Mohsin Abrar^{c,d}, Mahmoud A. Abdelhafiz^e, Xinbin Feng^{a,f,**}

^a State Key Laboratory of Environmental Geochemistry, Institute of Geochemistry, Chinese Academy of Sciences, Guiyang 550081, PR China

^b Department of Ecological Sciences and Engineering, College of Environment and Ecology, Chongqing University, Chongqing 400045, PR China

^c College of Resources and Environment, Zhongkai University of Agriculture and Engineering, 510225 Guangzhou, China

^d Engineering and Technology Research Center for Agricultural Land Pollution and Integrated Prevention, Guangzhou, China

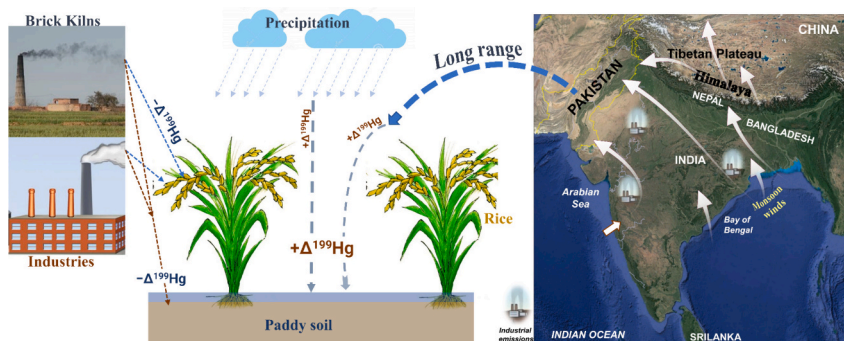
^e Geology Department, Faculty of Science, Al-Azhar University, Assiut 71524, Egypt

^f University of Chinese Academy of Sciences, Beijing 100049, PR China

HIGHLIGHTS

- The first study depicting Hg status, origin, and sources in paddy soils of Pakistan.
- Contaminated sites had negative to near-zero $\Delta^{199}\text{Hg}$ values due to local emissions.
- Uncontaminated sites exhibited $\Delta^{199}\text{Hg}$ values near-zero to positive.
- Positive $\Delta^{200}\text{Hg}$ values show wet precipitation as a major Hg input in study area.
- Long range transboundary Hg transport by Monsoon winds predominates in Pakistan.

GRAPHICAL ABSTRACT



ARTICLE INFO

Editor: Deyi Hou

Keywords:

Paddy soil
Pakistan
Hg stable isotopes
Transboundary Hg transport
South Asia

ABSTRACT

Mercury (Hg) is a globally distributed heavy metal. Here, we study Hg concentration and isotopic composition to understand the status of Hg pollution and its sources in Pakistan's paddy soil. The collected paddy soils ($n = 500$) across the country have an average THg concentration of 22.30 ± 21.74 ng/g. This low mean concentration suggests Hg pollution in Pakistan was not as severe as previously thought. Meanwhile, samples collected near brick kilns and industrial areas were significantly higher in THg than others, suggesting the influence of Hg emitted from point sources in certain areas. Soil physicochemical properties showed typical characteristic of mineral soils due to the study area's arid to semi-arid climate. Hg stable isotopes analysis, depicted mean $\Delta^{199}\text{Hg}$ of $-0.05 \pm 0.12\%$ and mean $\delta^{202}\text{Hg}$ of $-0.45 \pm 0.35\%$, respectively, for contaminated sites, depicting Hg was primarily sourced from coal combustion by local anthropogenic sources. While uncontaminated sites show mean $\Delta^{199}\text{Hg}$ of $0.15 \pm 0.08\%$, mean $\Delta^{200}\text{Hg}$ of $0.06 \pm 0.07\%$ and mean $\delta^{202}\text{Hg}$ of $-0.32 \pm 0.28\%$, implying long-range transboundary Hg transport through wet Hg(II) deposition as a dominant Hg source. This study fills a significant knowledge gap regarding the Hg pollution status in Pakistan and suggests that the Hg risk in Pakistan paddies is generally low.

* Corresponding author.

** Correspondence to: X. Feng, University of Chinese Academy of Sciences, Beijing, 100049, PR China.

E-mail addresses: mengbo@vip.skleg.cn (B. Meng), fengxinbin@vip.skleg.cn (X. Feng).

<https://doi.org/10.1016/j.scitotenv.2024.173879>

Received 28 March 2024; Received in revised form 31 May 2024; Accepted 7 June 2024

Available online 8 June 2024

0048-9697/© 2024 Elsevier B.V. All rights reserved, including those for text and data mining, AI training, and similar technologies.

1. Introduction

Hg is a pollutant of global concern owing to its long-range transport in the atmosphere and worldwide deposition to aquatic and terrestrial ecosystems via wet or dry pathways (Driscoll et al., 2013; Selin, 2009; Zhu et al., 2016). In aquatic ecosystems, microbial activities convert inorganic Hg species to methylmercury (MeHg), a potent neurotoxin that can accumulate up to 10^6 times in food chains (Mergler et al., 2007; Selin, 2009). Seafood (e.g., fish and other mammals) intake has been regarded as the major human MeHg exposure pathway (Houserova et al., 2007; Rothenberg et al., 2014; Trasande et al., 2016). Soil is the largest Hg reservoir globally (Wang et al., 2019). Inorganic Hg can also be methylated in terrestrial ecosystems by aerobes (Bishop et al., 2020; Feng et al., 2022; Shanley et al., 2020). Hence, a significant fraction of the MeHg approaching aquatic environments (streams, lakes, oceans) by erosion, runoff, or leaching has been formed in terrestrial landscapes (Bravo et al., 2017; Burns et al., 2014; Rodenhouse et al., 2019; Siddiqi, 2018). Rice paddies provide a favorable environment for microbial Hg methylation (Aslam et al., 2022; Meng et al., 2011). Rice plants can accumulate large amounts of MeHg during their growth (Aslam et al., 2022; Meng et al., 2010; Meng et al., 2012; Meng et al., 2014), and rice consumption could be another critical exposure source of MeHg in humans, especially inland populations who scarcely consume fish (Aslam et al., 2020; Feng et al., 2008; Zhang et al., 2010). As a result, the sources and fates of Hg in paddy soil should be carefully examined to enable further Hg pollution control.

Mercury isotope geochemistry provides a promising tool for understanding Hg's sources and fate in the environment (Blum et al., 2014; Kwon et al., 2020). The seven natural stable isotopes of Hg, with atomic mass ranging from 196 to 204, display both mass-dependant (MDF, represented as $\delta^{202}\text{Hg}$) and mass-independent fractionation (MIF, denoted as $\Delta^{199}\text{Hg}$, $\Delta^{200}\text{Hg}$ and $\Delta^{201}\text{Hg}$ values). Various biological, chemical, and physical processes can trigger the MDF of Hg isotopes. In comparison, the MIF of odd isotopes (^{199}Hg and ^{201}Hg) is limited to a few processes, such as aqueous Hg(II) photoreduction and MeHg photodegradation (Bergquist and Blum, 2009). The MIF of ^{200}Hg is possibly ascribed to the photochemical oxidation of gaseous Hg(0) species (Chen et al., 2012). Much more significant variations for $\delta^{202}\text{Hg}$ and $\Delta^{199}\text{Hg}$ (~10‰ for both) and $\Delta^{200}\text{Hg}$ (~1‰) were demonstrated in natural samples (Blum et al., 2014). Surface soils may have different Hg sources like precipitation (Dry or Wet), weathered rocks (geogenic origin), and litterfall exhibiting distinct MIF patterns (Wang et al., 2017). MIF of odd Hg isotopes is chiefly induced by the magnetic isotopes effect (MIE) or nuclear volume effect (NVE) (Blum et al., 2014; Jiskra et al., 2015; Yin et al., 2013b). Thus, MIF provides additional information on the specific processes in environmental matrices (Bergquist and Blum, 2007). However, no significant MIF ($\Delta^{199}\text{Hg} < 0.2\text{‰}$) has been observed in geogenic materials like mineral deposits, hydrothermal emissions, and volcanoes (Smith et al., 2005; Zambardi et al., 2009). Hence, MIF for geogenic samples (100% geological source) considers $\Delta^{199}\text{Hg} = 0.00\text{‰}$ (Yin et al., 2016a). A study conducted in a forest ecosystem found that MIF was observed on leaf surfaces due to photoreduction but not in soil (Demers et al., 2013). Similarly, histosols (high organic matter) in boreal coniferous forests depicted NVE occurrence, but this phenomenon could be limited (Jiskra et al., 2015). Therefore, pre-depositional processes from atmospheric inputs inducing $\Delta^{199}\text{Hg}$ shift in soils have been observed, while post-depositional processes are unlikely or insignificant (Wang et al., 2017; Zhang et al., 2013). Distinct Hg isotopic signals among natural and anthropogenic Hg emission sources have been published (Sun et al., 2019; Yin et al., 2016a), opening the possibility of using Hg isotopes for source tracing (Yin et al., 2013a; Zhang et al., 2013).

Soil Hg levels and their fate (accumulation, retention, bioavailability mobility, etc.) are determined by soil morphology and genesis as well as soil properties, including redox potential soil organic matter stability, content, texture, and pH (Abdelhafiz et al., 2023; Liu et al., 2022; Obrist

et al., 2011; Pu et al., 2022). The global Hg biogeochemical cycling is closely coupled with carbon cycling (Couic et al., 2018; Driscoll et al., 2013; Ravichandran, 2004); hence, total organic carbon (TOC) solely explains 46% variability in Hg concentrations of soils (Beckers and Rinklebe, 2017). Furthermore, Hg:TOC ratios are a useful normalized indicator of the influence of anthropogenic Hg releases on Hg enrichment in topsoil (Xue et al., 2019). Hg biogeochemical cycling in organic-rich soils like forest ecosystems is well studied and documented (Jiskra et al., 2015; Obrist, 2012; Wang et al., 2017; Zheng et al., 2016), but studies are scarce in arid and semi-arid regions delineating Hg cycling especially in mineral paddy soils.

Pakistan is the fourth largest rice exporting country globally, contributing 8.2% of rice globally (PBS, 2014). However, due to its rapid population growth, urbanization, and industrialization in past decades (Azizullah et al., 2011), anthropogenic Hg emissions (e.g., cement production, chloralkali plants, coal combustion, and domestic usage) increased rapidly, resulting in elevating environmental pressures (Ali et al., 2019; Eqani et al., 2016). Pakistan is situated in the neighborhood of China and India, the two largest Hg emitters in the world. Long range transboundary Hg transport facilitated by South Asian monsoon winds (Huang et al., 2023; Kang et al., 2016), could contribute significant amounts of Hg to Pakistan. The Minamata Convention on Hg consists of provisions for a global monitoring program and effectiveness evaluation to provide data on changes in mercury sources in various environmental matrices (Kwon et al., 2020). Although, knowledge of Hg exposure remains limited due to data unavailability in various regions and sub-populations (Basu et al., 2018). Furthermore, major challenges such as climate change (changes in precipitation patterns, surface temperature, biomass burning) (Friedli et al., 2009; Kumar et al., 2018; Mao et al., 2017; Perlinger et al., 2018; Sprovieri et al., 2017), and other human activities (urbanization and land use change) (Domagalski et al., 2016; Drevnick et al., 2016; Fleck et al., 2016), could interfere with the identification of Minamata convention relevant changes in Hg sources for establishing a globally comparable performance indicator that can discriminate between changes in Hg sources subject to regulation and distinguish other influences on Hg from the environment (Kwon et al., 2020). However, studies regarding Hg status and interactions in soils are lacking at national and regional level. To the best of our knowledge, current research is the first comprehensive large-scale study in rice paddies of arid to semi-arid regions regarding Hg. We believe this work will provide raw data for future studies dealing with Hg biogeochemical cycling in rice paddies under global change scenario. As, Pakistan is the most threatened by global warming and climate change in the South Asian region. Hence, it is urgent to investigate Hg's pollution status and sources in Pakistan paddy soil.

This study investigates Hg contents, Hg isotopic composition, and physicochemical parameters of paddy soil collected from the major rice growing provinces of Pakistan, with the aims of (1) assessing Hg contamination status in soil, (2) examining the prevailing geochemical factors influencing Hg distribution in soil, and (3) understanding potential Hg sources in soil.

2. Materials and methods

2.1. Study area and sample collection

In 2017, paddy soils ($n = 500$) were collected from two major rice-producing provinces in Pakistan, i.e., Punjab and Sindh (Fig. 1). These two provinces represent 92% of Pakistan's total rice-cultivated land (PBS, 2014). The Punjab is located in central eastern Pakistan and has sub-tropic and sub-humid climates with rainfall < 800 mm/year. Districts of northern Punjab are significant hubs of industrialization in the country, including facilities from small-scale cottages to large-scale industries. South Asian Monsoon (July–September) is responsible for $> 80\%$ of total annual precipitation in summer. Summer is long and hot, with a maximum temperature of 43 °C, followed by short winters, with a

minimum temperature of 4 °C. For this work, a total of 414 surface paddy soil samples (0–10 cm) were collected from sixteen (16) rice-growing districts of Punjab (Table S1). Sindh is the southern part of Pakistan. This province's climate is predominantly tropical to sub-

tropical in the lower and upper plains. Summers are characterized by hot and humid conditions, with temperatures reaching as high as 50 °C. On the other hand, winters are brief and mild in this province. Eighty-six (86) paddy soil samples were collected from six (6) districts in Sindh

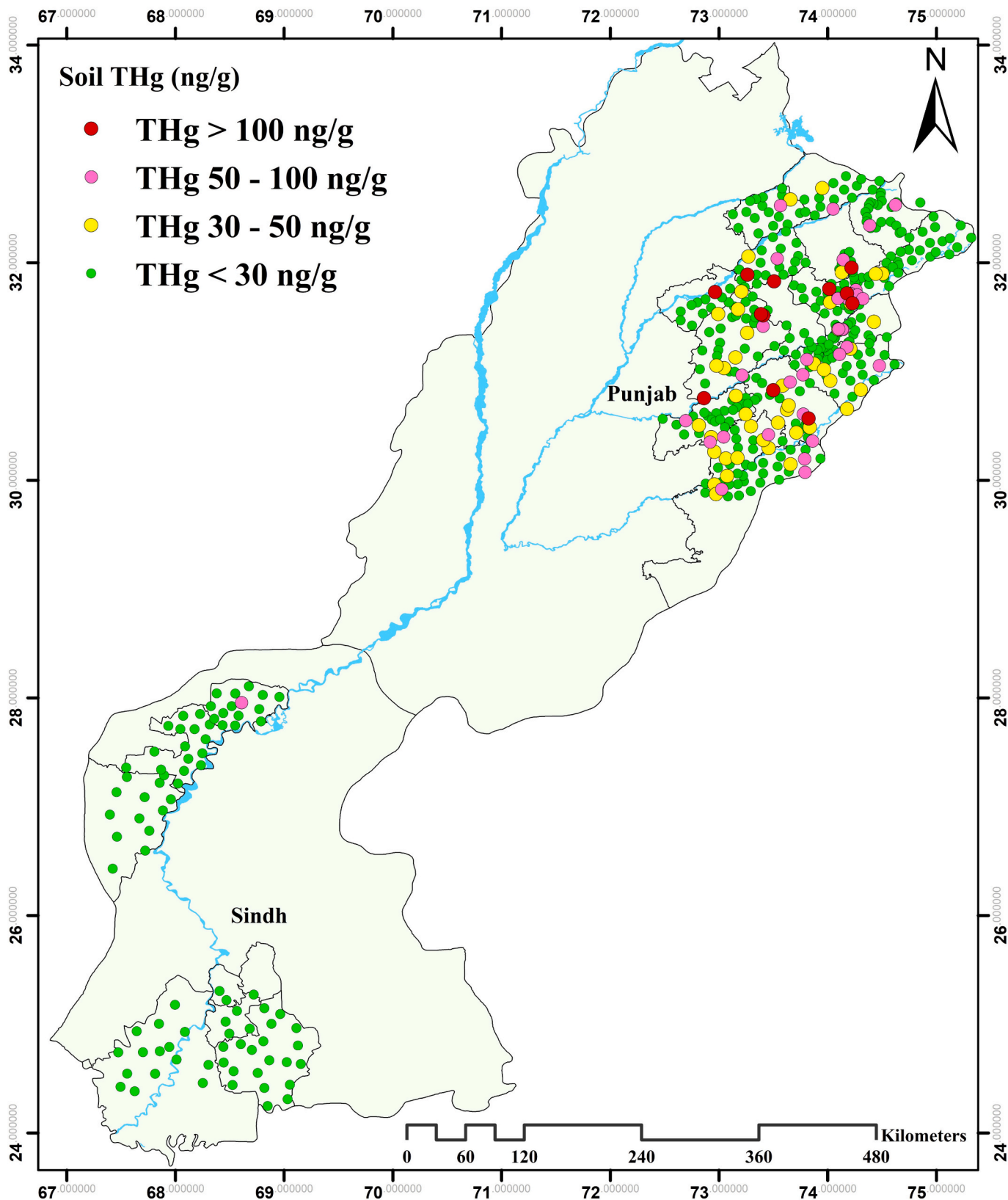


Fig. 1. Map showing locations and mercury concentrations determined in paddy soil samples ($n = 500$) from rice-growing areas of Pakistan.

(Table S1). Both contaminated and uncontaminated locations were sampled due to the large extent of the study area and the lack of Hg contamination data. All conventional Hg emission sources (brick kilns, wastewater effluent, chloralkali plants, industrial areas, coal-fired power plants, incinerators, etc.) were considered as contaminated sites. Paddy soil samples were collected at distances of 8–10 km to ensure uniform sampling densities across both contaminated and uncontaminated sites, except for two types of sites: chloralkali plant and coal-fired power plant. At brick kiln locations, samples were collected 100–120 m downwind from the brick kiln unit. Further details regarding soil types in the study area can be found in supplementary information (SI) section S1.1 and Table S1. The locations of the samples collected (Fig. 1) and the extent of sampling districts are given in Table S2.

2.2. Sample preparation and analytical methods

Sample preparation procedures involved in this study are mentioned in text section S1.2 of SI. To determine the total Hg (THg) concentration in soil, 0.2–0.4 g of each sample was digested in a water bath (95 °C) for an hour after adding 5 ml aqua regia (HCl: HNO₃ = 3:1, v/v). The digests were diluted to 25 ml using 18.2 MΩ-cm water and measured by Brooks Rand model III cold vapor atomic absorption fluorescence spectrophotometer (CVAFS) following a previous method (USEPA, 2002).

The selected digested samples were diluted to 0.5 ng/ml Hg concentration in 10–20% acid matrices for Hg isotopic composition analysis using a Neptune Plus multiple-collector inductively coupled plasma mass spectrometer, following a previous method (Yin et al., 2016b). Hg isotopic compositions were determined by standard-sample bracketing protocol (Bergquist and Blum, 2007), and MDF is reported as δ^xHg relative to NIST-3133 as follows:

$$\delta^x\text{Hg}(\text{‰}) = \left[\frac{(\text{}^x\text{Hg}/\text{}^{198}\text{Hg})_{\text{sample}}}{(\text{}^x\text{Hg}/\text{}^{198}\text{Hg})_{\text{NIST3133}}} - 1 \right] \times 1000 \quad (1)$$

where x refers to the mass number of each Hg isotope from 199 to 202. MIF is reported as Δ^xHg and was calculated as follows:

$$\Delta^{199}\text{Hg} = \delta^{199}\text{Hg} - 0.2520 \times \delta^{202}\text{Hg} \quad (2)$$

$$\Delta^{200}\text{Hg} = \delta^{200}\text{Hg} - 0.5024 \times \delta^{202}\text{Hg} \quad (3)$$

$$\Delta^{201}\text{Hg} = \delta^{201}\text{Hg} - 0.7520 \times \delta^{202}\text{Hg} \quad (4)$$

Soil CRM GSS-4 were determined before and after each analytical session and yielded values (δ²⁰²Hg = −1.80 ± 0.02‰, Δ¹⁹⁹Hg = −0.34 ± 0.07‰, Δ²⁰⁰Hg = 0.03 ± 0.06‰, Δ²⁰¹Hg = −0.44 ± 0.05‰, mean ± S.D, n = 4) similar with previously reported data (Bergquist and Blum, 2007; Wang et al., 2017). NIST-3177 secondary standard solutions, diluted to 0.5 ng/ml, were also measured and gained similar values to those recommended by Bergquist and Blum (2007).

EC and pH were determined in each sample using a portable combo meter (HI98130, Hanna Instruments, Italy), which had an accuracy of 0.001 pH units. The concentrations of total carbon (TC) and total nitrogen (TN) in the samples were determined by the CHNOS Elemental analyzer based on the combustion method (Elementar Analysensysteme GmbH, Germany). An elemental analyzer also determined the total inorganic carbon (TIC). Samples previously used for TC were placed in a porcelain crucible and burned in a muffle furnace at 500 °C for 4 h to remove all organic carbon (Wiesmeier et al., 2012). To calculate total organic carbon (TOC), TIC was subtracted from TC (Eq. 5).

$$\text{TOC} = \text{TC} - \text{TIC} \quad (5)$$

2.3. Quality assurance/quality control, statistical analysis, and geographical mapping

To analyze THg, the atomic fluorescence spectrometer (AFS) was

calibrated using standard solutions to get a standard curve. To ensure quality control, every tenth sample was triplicated, method blanks and certified reference materials were also analyzed. The method detection limits (3σ) for THg were determined to be 0.005 ng/g. Soil samples depicted relative standard deviation percentages (RSD%) for all triplicates < 7.84%. Similarly, every tenth soil sample was duplicated for C, N analysis yielded RSD% mean: 0.89% (Range: 0.05–2.99%). Measurements of GSS-5 and GSS-4 yielded Hg recoveries of 90–110%. Various CRM's GSS-5 (Soil) and GSS-4 (Soil) measured in the current study, including their analytical findings, are enlisted in Table S3. All acids used in the analyses were of ultrapure grade and analytical grade reagents (Sinopharm Chemical Reagent Co., Ltd., China). Prior to analyses, all labware, including glass containers, bubblers, tubes, and beakers, were washed rigorously using detergent and then thoroughly rinsed with deionized water (DI) and double-distilled water (DDW), respectively. After washing, glassware was preheated in a muffle furnace at 500 °C (2 h) to obtain very low Hg blanks.

THg concentration data were statistically analyzed by Sigma Plot (Version 14, Systat Software Inc., USA). Using descriptive statistics, Hg values are depicted as mean ± standard deviation (SD). Principal Component Analysis (PCA) was employed to evaluate the spatial correlation and similarity of the eigenvectors (parameters) with the factor scores of different groups. One-way analysis of variance (ANOVA) was used to calculate significant differences among different groups means. To determine significant differences between two groups means t-test was also applied. Correlation coefficients (r) and significance of probabilities (p) were also determined using Pearson correlation. A GPS module (Monterra, Garmin, USA) was employed to record latitudes and longitudes of sampled locations. These locations were then subjected to ArcGIS version 10.5 software (ESRI, USA) for producing geographical maps.

3. Results and discussion

3.1. Spatial distribution of THg in paddy soils

Mercury contents of collected soil samples (n = 500) are presented in Fig. 1. Despite four (04) outliers showing extremely high THg contents (455 to 12,689 ng/g), most samples (n = 496) show much lower THg contents ranging from 5.42 to 199 ng/g, with the mean value of 22.30 ± 21.74 ng/g. These four (04) outliers were potentially polluted by point Hg sources and were precluded from statistical analyses to avoid misinterpretation. Following this act, the highest mean THg concentrations were found in Okara (mean: 35.90 ± 27.52 ng/g) and Sheikhpura (mean: 35.32 ± 37.13 ng/g) districts of the Punjab. Relatively higher soil THg mean values were found in Punjab (27.11 ± 30.19 ng/g) than in Sindh (12.10 ± 5.58 ng/g) (Fig. S1). As a whole, the mean THg concentration of paddy soils (22.30 ± 21.74 ng/g) depicting three times lower than the mean background THg concentrations in Chinese soil (65 ng/g) (Shifaw, 2018; Wang et al., 2016), and is far lower than the recommended threshold limits of Hg in agricultural soils of China (600 ng/g, 6.5 < pH ≤ 7.5; 1000 ng/g, pH > 7.5) (GB15618, 2018) and European Union (500 ng/g) (Jarva, 2016; Tóth et al., 2016).

Although, our results suggest that paddy soils in Pakistan are at low risk in terms of mean THg concentration, the influence of anthropogenic activities can still be revealed in our samples by looking at our data in detail. Specifically, 91 % (n = 455) of analyzed soil samples had THg < 50 ng/g, 7 % of samples (n = 34) were measured in THg concentrations > 50–100 ng/g, and 2 % of samples (n = 8) exceeded the THg concentration of 100 ng/g. We compared soil THg concentrations among three sampling groups (brick kiln, industrial, and non-point source locations) (Fig. S2). Analysis of variance (ANOVA) revealed significantly higher mean THg concentrations in soil samples from Industrial (34.90 ± 33.08 ng/g) and Brick kilns (37.36 ± 43.75 ng/g) sampling sites than others without any obvious Hg point source (19.10 ± 13.23 ng/g) (p < 0.05) (Table S4). We found that soil samples exceeding 100 ng/g were

collected around brick kilns or industrial zones. Brick kilns consume large volumes of coal during production, and burning coal releases Hg to the ambient environment. Our previous study in similar rice-growing areas of Pakistan also depicted brick kilns as a prominent Hg source of rice grains (Aslam et al., 2020).

3.2. Soil physicochemical parameters

Soil physicochemical parameters determined in our study are given in Table S5. While projection of vectors of variables with scores on the three main axes of the principal components are shown in Fig. S3. PC1 explains 38.8% variance with eigen value of 2.72 while PC2 explains 20.2% variance. The first two components explain 60% of variance together. All principal components and their factor loadings with eigen values are given (Table S6).

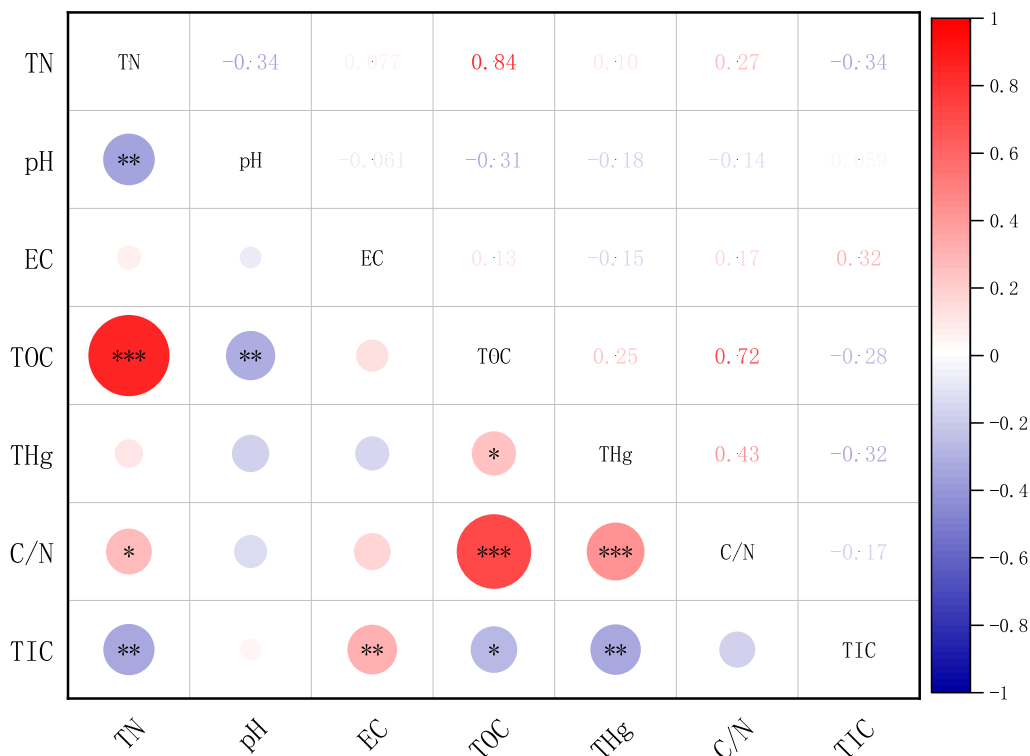
The mean pH obtained in this study is 7.89 ± 0.32 (Range: 6.75 to 8.72). The reasons for this alkaline pH in Pakistan are: a). calcareous parent material b). low rainfall, c). low forest density, d). arid to semi-arid climate. The soil parent material produces Ca^{2+} , Mg^{2+} , Na^+ , CO_3^{2-} , HCO_3^- , SO_4^{2-} and more OH^- than H^+ ions in the soil solution. In soils with low organic matter, Hg(II) is mainly bound to mineral soil components (Biester et al., 2002), so more reactive and prone to methylation (Skylberg et al., 2006). On the contrary, high clay content, strongly alkaline conditions, and low organic matter content favored soil retaining Hg(II) species (Šípková et al., 2016). However, due to the complex chemistry of Hg, general statements about Hg species mobility are challenging. No correlation was obtained between soil THg contents and pH (Fig. 2) due to the narrow pH range indicating more similar soil parent material and climate in the study area (Table S1). The mean TN and TOC contents of the collected soils were 1.02 ± 0.37 mg/g and 9.69 ± 12.17 mg/g respectively, representing mineral soils (organic matter < 1%). No significant relationship was found between THg and TN

contents of paddy soil. A weaker but positive relationship ($r = 0.25$, $p \leq 0.05$) was found for THg and TOC contents of soil, which could be due to the adsorption of Hg species by soil organic matter (Fig. 2).

The mean C/N ratio of 8.87 ± 7.23 (Range: 4.11–69.31) was determined in the studied paddy soil. A positive correlation between THg and C/N ratio ($r = 0.43$, $p \leq 0.001$) (Fig. 2) is observed in our study, which implies that with an increasing C/N ratio, the THg contents would also be increased (O’Driscoll et al., 2011; Obrist, 2012). In other words, mineralization will decrease THg contents, and immobilization provides more carbon stock to bind Hg (Abrar et al., 2021; Ravichandran, 2004; Skylberg et al., 2006). These low C/N ratios are attributed to arid to semi-arid climates, higher temperatures, low rainfall, and very low organic matter. This may explain why low soil THg concentrations were found in the current study. Low or narrow C/N ratios could hinder the Hg buildup in the paddy soils, and unbound Hg may be leached down or evaded back after reduction to the atmosphere (Obrist et al., 2011). Combined with the discussion in Section 3.1, our results suggest that the distribution of THg in Pakistan paddy soils is a net effect of anthropogenic and soil physicochemical processes.

3.3. Hg sources revealed by Hg isotopes

Thirty samples were selected for Hg isotopic analysis (Fig. 3). They were further classified as contaminated and uncontaminated soil based on presence of Hg source at sampling site. Contaminated soils had the highest THg mean concentration, 326 ± 3688 ng/g and were collected around brick kilns ($n = 7$), chloralkali ($n = 3$), and industrial zones ($n = 2$). They have mean $\Delta^{199}Hg$ values of $-0.05 \pm 0.12\%$ and $\delta^{202}Hg$ of $-0.45 \pm 0.35\%$. On the other hand, uncontaminated soils have the lower mean Hg of 40.61 ± 25.42 ng/g and were collected from areas without known point Hg emission sources. They display relatively higher mean $\Delta^{199}Hg$ values of $0.15 \pm 0.08\%$ and $\delta^{202}Hg$ values of -0.32



* $p < 0.05$ ** $p < 0.01$ *** $p < 0.001$

Fig. 2. Heat map depicting correlations among paddy soil THg and physicochemical parameters.

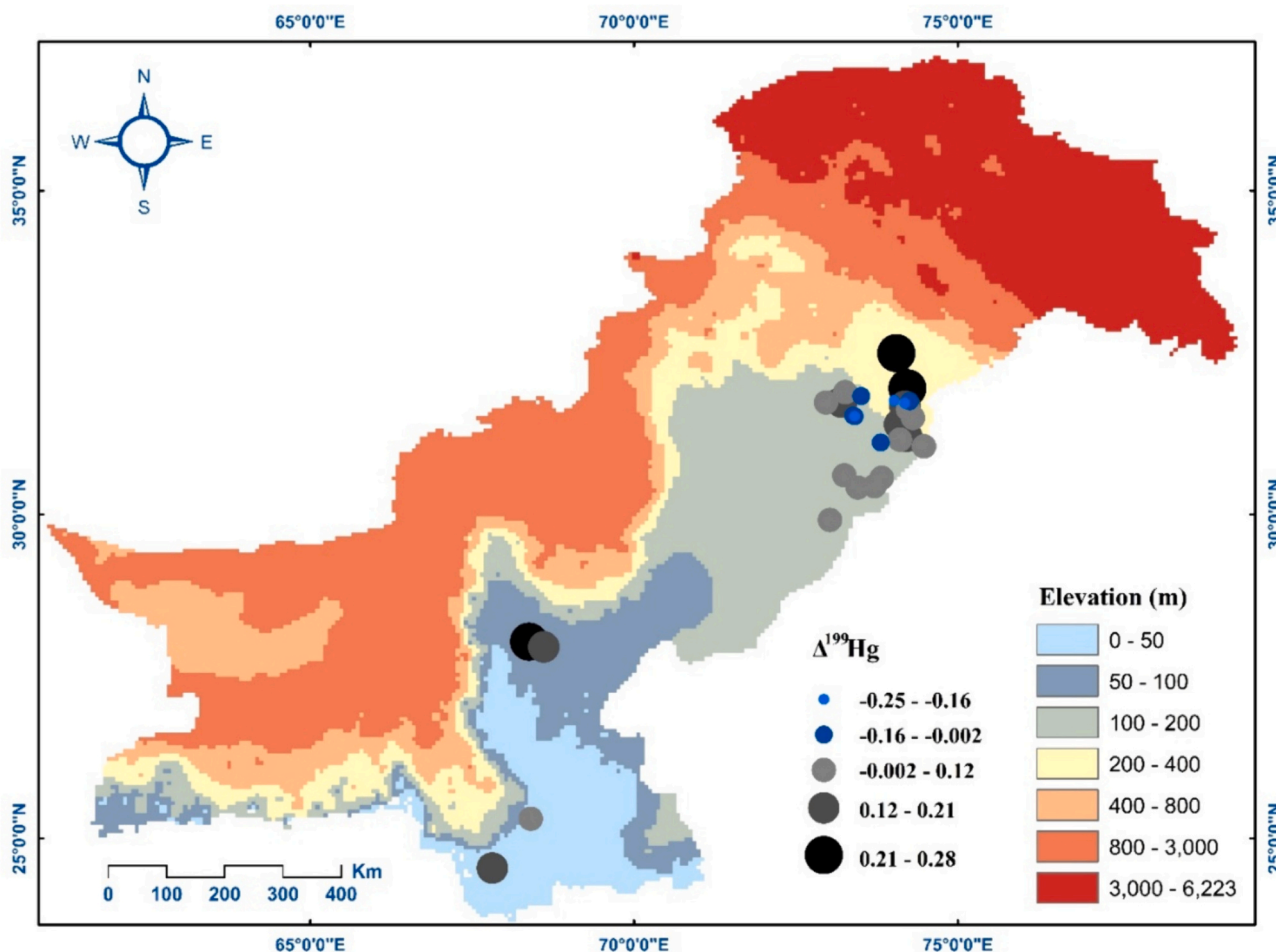


Fig. 3. Map showing sampling locations of Hg stable isotopes paddy soil samples, elevation gradient, and occurrence of $\Delta^{199}\text{Hg}$ in the study area.

$\pm 0.28\text{‰}$ (Table S7). Overall, the results of this study fall into the range of samples collected from various sites across the globe (Fig. 4). Hg isotopic signature in the soil provides insights into the region's Hg sources. As shown in Fig. 4, samples from contaminated sites (mostly brick kilns) fall in the proximity of coal (Biswas et al., 2008; Sherman et al., 2012; Sun et al., 2014). Although data is unavailable regarding the Hg stable isotopic composition of Pakistani coal, the Hg stable isotope signatures obtained here are similar to that reported for flue gas emitted from coal combustion in China ($\Delta^{199}\text{Hg}$: $-0.10 \pm 0.14\text{‰}$ (-0.13 to 0.1‰); $\delta^{202}\text{Hg}$: $-2.54 \pm 0.62\text{‰}$ (-3.01 to -1.38‰) (Li et al., 2021) and feed coal ($\delta^{202}\text{Hg}$: $-1.38 \pm 0.42\text{‰}$; $\Delta^{199}\text{Hg}$: $-0.03 \pm 0.06\text{‰}$) (Song et al., 2021). Yin et al. (2014) found that Hg^0 emissions from coal combustion could have $\delta^{202}\text{Hg}$ of $\sim -0.70\text{‰}$ and $\Delta^{199}\text{Hg}$ of $\sim -0.05\text{‰}$, which are comparable with our results on contaminated soil. This confirms our early hypothesis that coal combustion in brick kilns is an important Hg pollution source in the paddy fields of Pakistan.

Non-contaminated sites depicted different $\Delta^{199}\text{Hg}$ but similar $\delta^{202}\text{Hg}$ signatures to contaminated sites. The $\delta^{202}\text{Hg}$ values give a poor constraint on Hg sources, given that Hg MDF can arise due to diverse physical, biological, and chemical processes (Blum et al., 2014). The mean positive $\Delta^{199}\text{Hg}$ ($0.15 \pm 0.08\text{‰}$), however, may suggest that Hg was primarily sourced via atmospheric Hg(II) wet deposition (Fig. 4), given that precipitation samples display positive $\Delta^{199}\text{Hg}$ values (Chen et al., 2012; Gratz et al., 2010; Sherman et al., 2012). Similarly, positive $\Delta^{199}\text{Hg}$ values were generally observed for long-range transported Hg derived from Indian emissions (Huang et al., 2020; Wang et al., 2015; Yuan et al., 2015). As positive $\Delta^{199}\text{Hg}$ MIF anomalies influenced by atmospheric photoreduction, large values of $\Delta^{199}\text{Hg}$ can represent an

extensive fractionation process in water droplets due to long-range transboundary transportation (Chen et al., 2012; Gratz et al., 2010; Wang et al., 2015). More similar $\Delta^{199}\text{Hg}$ values to our work have been reported in frozen soil samples (Mean: -0.07 ± 0.50 ; Range: -0.45 to 0.24‰) (Huang et al., 2020), lake sediments (Mean: 0.07 to 0.44‰) (Huang et al., 2023) and (Mean: $-0.10 \pm 0.10\text{‰}$) in TGM (Yu et al., 2022) at the Tibetan Plateau. To grow rice plants, irrigation of paddy fields is necessary and requires large volumes of water that contain abundant Hg sourced from precipitation. A previous study also observed positive $\Delta^{199}\text{Hg}$ values ($0.30 \pm 0.12\text{‰}$; $n = 27$) in watershed soil impacted by rainfall (Lepak et al., 2015). Interestingly, even MIF values $\Delta^{200}\text{Hg}$ (Mean: 0.06 ± 0.07 ; Range: -0.05 to 0.18‰) determined at uncontaminated sites were significantly more positive (t -test, $p < 0.01$) (Table S8) than those at contaminated sites (Mean: -0.03 ± 0.07 ; Range: -0.12 to 0.07‰), which also agree with previous results on precipitation at Lhasa (Mean: 0.13‰) (Yuan et al., 2015), and in lake sediments at the Tibetan Plateau (0.03 to 0.08‰) (Huang et al., 2023). Overall, the results of this study suggest that in addition to local point Hg emission sources, a substantial amount of Hg in paddy soil comes from wet Hg(II) deposition.

4. Conclusions and implications

This study provides a novel set of data regarding the Hg concentration and isotopic composition in Pakistan's paddy soil and reveals that (1) Hg pollution in Pakistan's soil was not as severe as previously thought, (2) despite a few soils that were contaminated by local anthropogenic emissions, most soils receive Hg mainly from wet

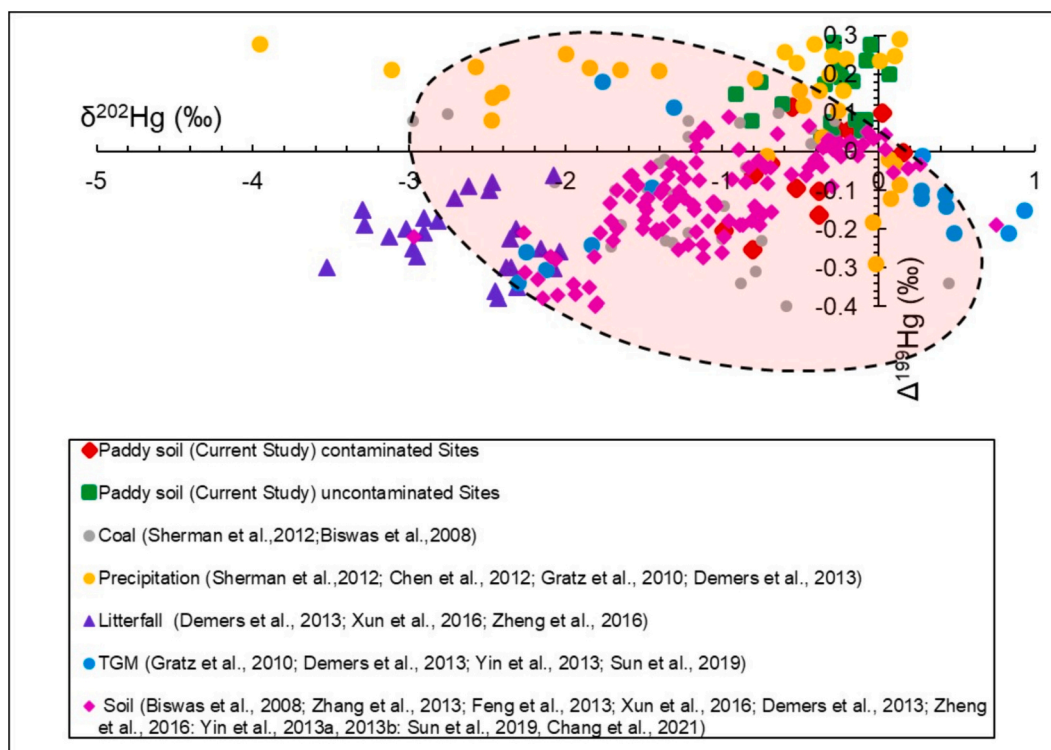


Fig. 4. $\delta^{202}\text{Hg}$ (‰) vs $\Delta^{199}\text{Hg}$ (‰) for the current study in paddy soils across Pakistan and comparison among previous studies from other parts of the world. The light pink circled field represents Hg stable isotopes of coal observed from significant coal-producing regions worldwide (taken from Sun et al., 2014).

deposition and are very pristine. Rice grown in Pakistan paddies, thus, should have low Hg risks, as supported by a recent study (Aslam et al., 2020).

CRedit authorship contribution statement

Muhammad Wajahat Aslam: Writing – original draft, Visualization, Methodology, Formal analysis, Data curation. **Bo Meng:** Writing – review & editing, Supervision, Resources, Funding acquisition, Conceptualization. **Waqar Ali:** Methodology, Formal analysis, Data curation. **Muhammad Mohsin Abrar:** Writing – review & editing, Visualization, Methodology, Formal analysis, Data curation. **Mahmoud A. Abdelhafiz:** Writing – review & editing, Visualization, Methodology, Formal analysis, Data curation. **Xinbin Feng:** Writing – review & editing, Supervision, Resources, Funding acquisition, Conceptualization.

Declaration of competing interest

The authors declare that they have no known competing financial interests or personal relationships that could have appeared to influence the work reported in this paper.

Data availability

Data will be made available on request.

Acknowledgments

This study was funded by the National Natural Science Foundation of China (41931297) and the CAS “Light of West China” program. The authors thank Runsheng Yin for technical assistance regarding Hg isotope analysis, critical review, and editing. We also thank Hivox (Pvt.) Ltd. for providing logistic support during the sample collection campaign in Pakistan.

Appendix A. Supplementary data

Supplementary data to this article can be found online at <https://doi.org/10.1016/j.scitotenv.2024.173879>.

References

- Abdelhafiz, M.A., Liu, J., Jiang, T., Pu, Q., Aslam, M.W., Zhang, K., et al., 2023. DOM influences Hg methylation in paddy soils across a Hg contamination gradient. *Environ. Pollut.* 121237.
- Abrar, M.M., Xu, H., Aziz, T., Sun, N., Mustafa, A., Aslam, M.W., et al., 2021. Carbon, nitrogen, and phosphorus stoichiometry mediate sensitivity of carbon stabilization mechanisms along with surface layers of a Mollisol after long-term fertilization in Northeast China. *J. Soil. Sediment.* 21, 705–723.
- Ali, W., Junaid, M., Aslam, M.W., Ali, K., Rasool, A., Zhang, H., 2019. A review on the status of mercury pollution in Pakistan: sources and impacts. *Arch. Environ. Contam. Toxicol.* 1–9.
- Aslam, M.W., Ali, W., Meng, B., Abrar, M.M., Lu, B., Qin, C., et al., 2020. Mercury contamination status of rice cropping system in Pakistan and associated health risks. *Environ. Pollut.* 114625.
- Aslam, M.W., Meng, B., Abdelhafiz, M.A., Liu, J., Feng, X., 2022. Unravelling the interactive effect of soil and atmospheric mercury influencing mercury distribution and accumulation in the soil-rice system. *Sci. Total Environ.* 803, 149967.
- Azizullah, A., Khattak, M.N.K., Richter, P., Häder, D.-P., 2011. Water pollution in Pakistan and its impact on public health—a review. *Environ. Int.* 37, 479–497.
- Basu, N., Horvat, M., Evers, D.C., Zastenskaya, I., Weihe, P., Tempowski, J., 2018. A state-of-the-science review of mercury biomarkers in human populations worldwide between 2000 and 2018. *Environ. Health Perspect.* 126, 106001.
- Beckers, F., Rinklebe, J., 2017. Cycling of mercury in the environment: sources, fate, and human health implications: a review. *Crit. Rev. Environ. Sci. Technol.* 47, 693–794.
- Bergquist, B.A., Blum, J.D., 2007. Mass-dependent and independent fractionation of Hg isotopes by photoreduction in aquatic systems. *Science* 318, 417–420.
- Bergquist, B.A., Blum, J.D., 2009. The odds and evens of mercury isotopes: applications of mass-dependent and mass-independent isotope fractionation. *Elements* 5, 353–357.
- Biester, H., Müller, G., Schöler, H., 2002. Estimating distribution and retention of mercury in three different soils contaminated by emissions from chlor-alkali plants: part I. *Sci. Total Environ.* 284, 177–189.
- Bishop, K., Shanley, J.B., Riscassi, A., de Wit, H.A., Eklöf, K., Meng, B., et al., 2020. Recent advances in understanding and measurement of mercury in the environment: terrestrial Hg cycling. *Sci. Total Environ.* 721, 137647.
- Biswas, A., Blum, J.D., Bergquist, B.A., Keeler, G.J., Xie, Z., 2008. Natural mercury isotope variation in coal deposits and organic soils. *Environ. Sci. Technol.* 42, 8303–8309.

- Blum, J.D., Sherman, L.S., Johnson, M.W., 2014. Mercury isotopes in earth and environmental sciences. *Annu. Rev. Earth Planet. Sci.* 42, 249–269.
- Bravo, A.G., Bouchet, S., Tolu, J., Björn, E., Mateos-Rivera, A., Bertilsson, S., 2017. Molecular composition of organic matter controls methylmercury formation in boreal lakes. *Nat. Commun.* 8, 14255.
- Burns, D.A., Nystrom, E.A., Wolock, D.M., Bradley, P.M., Riva-Murray, K., 2014. An empirical approach to modeling methylmercury concentrations in an Adirondack stream watershed. *J. Geophys. Res. Biogeo.* 119, 1970–1984.
- Chen, J., Hintelmann, H., Feng, X., Dimock, B., 2012. Unusual fractionation of both odd and even mercury isotopes in precipitation from Peterborough, ON, Canada. *Geochimica et Cosmochimica Acta* 90, 33–46.
- Couic, E., Grimaldi, M., Alphonse, V., Baland-Bolou-Bi, C., Livet, A., Giusti-Miller, S., et al., 2018. Mercury behaviour and C, N, and P biogeochemical cycles during ecological restoration processes of old mining sites in French Guiana. *Environ. Sci.: Processes Impacts* 20, 657–672.
- Demers, J.D., Blum, J.D., Zak, D.R., 2013. Mercury isotopes in a forested ecosystem: implications for air-surface exchange dynamics and the global mercury cycle. *Global Biogeochem. Cycles* 27, 222–238.
- Domagalski, J., Majewski, M.S., Alpers, C.N., Eckley, C.S., Eagles-Smith, C.A., Schenk, L., et al., 2016. Comparison of mercury mass loading in streams to atmospheric deposition in watersheds of Western North America: evidence for non-atmospheric mercury sources. *Sci. Total Environ.* 568, 638–650.
- Drevnick, P.E., Cooke, C.A., Barraza, D., Blais, J.M., Coale, K.H., Cumming, B.F., et al., 2016. Spatiotemporal patterns of mercury accumulation in lake sediments of western North America. *Sci. Total Environ.* 568, 1157–1170.
- Driscoll, C.T., Mason, R.P., Chan, H.M., Jacob, D.J., Pirrone, N., 2013. Mercury as a global pollutant: sources, pathways, and effects. *Environ. Sci. Technol.* 47, 4967–4983.
- Eqani, S.A.M.A.S., Bhowmik, A.K., Qamar, S., Shah, S.T.A., Sohail, M., Mulla, S.I., et al., 2016. Mercury contamination in deposited dust and its bioaccumulation patterns throughout Pakistan. *Sci. Total Environ.* 569, 585–593.
- Feng, P., Xiang, Y., Cao, D., Li, H., Wang, L., Wang, M., et al., 2022. Occurrence of methylmercury in aerobic environments: evidence of mercury bacterial methylation based on simulation experiments. *J. Hazard. Mater.* 438, 129560.
- Feng, X., Li, P., Qiu, G., Wang, S., Li, G., Shang, L., et al., 2008. Human exposure to methylmercury through rice intake in mercury mining areas, Guizhou Province, China. *Environmental science & technology* 42, 326–332.
- Fleck, J.A., Marvin-DiPasquale, M., Eagles-Smith, C.A., Ackerman, J.T., Lutz, M.A., Tate, M., et al., 2016. Mercury and methylmercury in aquatic sediment across western North America. *Sci. Total Environ.* 568, 727–738.
- Friedli, H.R., Arellano, A.F., Cinnirella, S., Pirrone, N., 2009. Mercury emissions from global biomass burning: spatial and temporal distribution. Mercury fate and transport in the global atmosphere: emissions. *Measurements and Models* 193–220.
- GB15618. Soil Environmental Quality Risk Control Standard for Soil Contamination of Agricultural Land In: Ecology Mo, Environment, editors. China Environmental Science Press Beijing, China, 2018.**
- Gratz, L.E., Keeler, G.J., Blum, J.D., Sherman, L.S., 2010. Isotopic composition and fractionation of mercury in Great Lakes precipitation and ambient air. *Environ. Sci. Technol.* 44, 7764–7770.
- Houserova, P., Kubán, V., Kráčmar, S., Sitko, J., 2007. Total mercury and mercury species in birds and fish in an aquatic ecosystem in the Czech Republic. *Environ. Pollut.* 145, 185–194.
- Huang, J., Kang, S., Yin, R., Guo, J., Lepak, R., Mika, S., et al., 2020. Mercury isotopes in frozen soils reveal transboundary atmospheric mercury deposition over the Himalayas and Tibetan plateau. *Environ. Pollut.* 256, 113432.
- Huang, J., Kang, S., Feng, X., Tang, W., Ram, K., Guo, J., et al., 2023. Northward extent of atmospheric mercury transboundary transport to the Himalayas and Tibetan plateau region. *Geophys. Res. Lett.* 50 e2022GL100948.
- Jarva, J., 2016. Geochemical Baselines in the Assessment of Soil Contamination in Finland.
- Jiskra, M., Wiederhold, J.G., Skyllberg, U., Kronberg, R.-M., Hajdas, I., Kretzschmar, R., 2015. Mercury deposition and re-emission pathways in boreal forest soils investigated with hg isotope signatures. *Environ. Sci. Technol.* 49, 7188–7196.
- Kang, S., Huang, J., Wang, F., Zhang, Q., Zhang, Y., Li, C., et al., 2016. Atmospheric mercury depositional chronology reconstructed from lake sediments and ice core in the Himalayas and Tibetan plateau. *Environ. Sci. Technol.* 50, 2859–2869.
- Kumar, A., Wu, S., Huang, Y., Liao, H., Kaplan, J.O., 2018. Mercury from wildfires: global emission inventories and sensitivity to 2000–2050 global change. *Atmos. Environ.* 173, 6–15.
- Kwon, S.Y., Blum, J.D., Yin, R., Tsui, M.T.-K., Yang, Y.H., Choi, J.W., 2020. Mercury stable isotopes for monitoring the effectiveness of the Minamata convention on mercury. *Earth Sci. Rev.* 203, 103111.
- Lepak, R.F., Yin, R., Krabbenhoft, D.P., Ogorek, J.M., DeWild, J.F., Holsen, T.M., et al., 2015. Use of stable isotope signatures to determine mercury sources in the Great Lakes. *Environ. Sci. Technol. Lett.* 2, 335–341.
- Li, X., Li, Z., Chen, J., Zhang, L., Yin, R., Sun, G., et al., 2021. Isotope signatures of atmospheric mercury emitted from residential coal combustion. *Atmos. Environ.* 246, 118175.
- Liu, J., Lu, B., Poulain, A.J., Zhang, R., Zhang, T., Feng, X., et al., 2022. The underappreciated role of natural organic matter bound hg (II) and nanoparticulate HgS as substrates for methylation in paddy soils across a hg concentration gradient. *Environ. Pollut.* 292, 118321.
- Mao, H., Ye, Z., Driscoll, C., 2017. Meteorological effects on hg wet deposition in a forested site in the Adirondack region of New York during 2000–2015. *Atmos. Environ.* 168, 90–100.
- Meng, B., Feng, X., Qiu, G., Cai, Y., Wang, D., Li, P., et al., 2010. Distribution patterns of inorganic mercury and methylmercury in tissues of rice (*Oryza sativa* L.) plants and possible bioaccumulation pathways. *J. Agric. Food Chem.* 58, 4951–4958.
- Meng, B., Feng, X., Qiu, G., Liang, P., Li, P., Chen, C., et al., 2011. The process of methylmercury accumulation in rice (*Oryza sativa* L.). *Environ. Sci. Technol.* 45, 2711–2717.
- Meng, B., Feng, X., Qiu, G., Wang, D., Liang, P., Li, P., et al., 2012. Inorganic mercury accumulation in rice (*Oryza sativa* L.). *Environ. Toxicol. Chem.* 31, 2093–2098.
- Meng, M., Li, B., Shao, J.-j., Wang, T., He, B., Shi, J.-b., et al., 2014. Accumulation of total mercury and methylmercury in rice plants collected from different mining areas in China. *Environ. Pollut.* 184, 179–186.
- Mergler, D., Anderson, H.A., Chan, L.H.M., Mahaffey, K.R., Murray, M., Sakamoto, M., et al., 2007. Methylmercury exposure and health effects in humans: a worldwide concern. *AMBIO: a journal of the human environment* 36, 3–11.
- Obrist, D., 2012. Mercury distribution across 14 US forests. Part II: patterns of methyl mercury concentrations and areal mass of total and methyl mercury. *Environ. Sci. Technol.* 46, 5921–5930.
- Obrist, D., Johnson, D., Lindberg, S., Luo, Y., Hararuk, O., Bracho, R., et al., 2011. Mercury distribution across 14 US forests. Part I: spatial patterns of concentrations in biomass, litter, and soils. *Environ. Sci. Technol.* 45, 3974–3981.
- O'Driscoll, N.J., Canário, J., Crowell, N., Webster, T., 2011. Mercury speciation and distribution in coastal wetlands and tidal mudflats: relationships with Sulphur speciation and organic carbon. *Water Air Soil Pollut.* 220, 313–326.
- PBS, 2014. Agricultural statistics of Pakistan area and production of important crops. Pakistan bureau of Statistics, p. 58. Statistical Year book.
- Perlinger, J.A., Urban, N.R., Giang, A., Selin, N.E., Hendricks, A.N., Zhang, H., et al., 2018. Responses of deposition and bioaccumulation in the Great Lakes region to policy and other large-scale drivers of mercury emissions. *Environ. Sci.: Processes Impacts* 20, 195–209.
- Pu, Q., Zhang, K., Poulain, A.J., Liu, J., Zhang, R., Abdelhafiz, M.A., et al., 2022. Mercury drives microbial community assembly and ecosystem multifunctionality across a hg contamination gradient in rice paddies. *J. Hazard. Mater.* 435, 129055.
- Ravichandran, M., 2004. Interactions between mercury and dissolved organic matter—a review. *Chemosphere* 55, 319–331.
- Rodenhouse, N.L., Lowe, W.H., Gebauer, R.L., McFarland, K.P., Bank MS, 2019. Mercury bioaccumulation in temperate forest food webs associated with headwater streams. *Sci. Total Environ.* 665, 1125–1134.
- Rothenberg, S.E., Windham-Myers, L., Creswell, J.E., 2014. Rice methylmercury exposure and mitigation: a comprehensive review. *Environ. Res.* 133, 407–423.
- Selin, N.E., 2009. Global biogeochemical cycling of mercury: a review. *Annu. Rev. Env. Resour.* 34, 43–63.
- Shanley, J.B., Marvin-DiPasquale, M., Lane, O., Arendt, W., Hall, S., McDowell, W.H., 2020. Resolving a paradox—high mercury deposition, but low bioaccumulation in northeastern Puerto Rico. *Ecotoxicology* 29, 1207–1220.
- Sherman, L.S., Blum, J.D., Keeler, G.J., Demers, J.D., Dvorchak, J.T., 2012. Investigation of local mercury deposition from a coal-fired power plant using mercury isotopes. *Environ. Sci. Technol.* 46, 382–390.
- Shifaw, E., 2018. Review of heavy metals pollution in China in agricultural and urban soils. *Journal of Health and Pollution* 8, 180607.
- Siddiqi, Z.M., 2018. Transport and fate of mercury (Hg) in the environment: need for continuous monitoring. In: Hussain, C. (Ed.), *Handbook of Environmental Materials Management*. Springer, Cham, Switzerland, pp. 1–20. Ed.
- Šípková, A., Száková, J., Hanč, A., Tlustoš, P., 2016. Mobility of mercury in soil as affected by soil physicochemical properties. *J. Soil. Sediment.* 16, 2234–2241.
- Skyllberg, U., Bloom, P.R., Qian, J., Lin, C.-M., Bleam, W.F., 2006. Complexation of mercury (II) in soil organic matter: EXAFS evidence for linear two-coordination with reduced sulfur groups. *Environ. Sci. Technol.* 40, 4174–4180.
- Smith, C.N., Kesler, S.E., Br, Klaue, Blum, J.D., 2005. Mercury isotope fractionation in fossil hydrothermal systems. *Geology* 33, 825–828.
- Song, Z., Wang, C., Ding, L., Chen, M., Hu, Y., Li, P., et al., 2021. Soil mercury pollution caused by typical anthropogenic sources in China: evidence from stable mercury isotope measurement and receptor model analysis. *J. Clean. Prod.* 288, 125687.
- Sprovieri, F., Pirrone, N., Bencardino, M., d'Amore, F., Angot, H., Barbante, C., et al., 2017. Five-year records of mercury wet deposition flux at GMOS sites in the northern and southern hemispheres. *Atmos. Chem. Phys.* 17, 2689–2708.
- Sun, R., Sonke, J.E., Heimbürger, L.-E., Belkin, H.E., Liu, G., Shome, D., et al., 2014. Mercury stable isotope signatures of world coal deposits and historical coal combustion emissions. *Environ. Sci. Technol.* 48, 7660–7668.
- Sun, R., Jiskra, M., Amos, H.M., Zhang, Y., Sunderland, E.M., Sonke, J.E., 2019. Modelling the mercury stable isotope distribution of earth surface reservoirs: implications for global hg cycling. *Geochim. Cosmochim. Acta* 246, 156–173.
- Tóth, G., Hermann, T., Da Silva, M., Montanarella, L., 2016. Heavy metals in agricultural soils of the European Union with implications for food safety. *Environ. Int.* 88, 299–309.
- Trasande, L., DiGangi, J., Evers, D.C., Petrlik, J., Buck, D.G., Šamánek, J., et al., 2016. Economic implications of mercury exposure in the context of the global mercury treaty: hair mercury levels and estimated lost economic productivity in selected developing countries. *J. Environ. Manage.* 183, 229–235.
- Wang, S., Zhong, T., Chen, D., Zhang, X., 2016. Spatial distribution of mercury (hg) concentration in agricultural soil and its risk assessment on food safety in China. *Sustainability* 8, 795.
- Wang, X., Luo, J., Yin, R., Yuan, W., Lin, C.-J., Sommar, J., et al., 2017. Using mercury isotopes to understand mercury accumulation in the montane forest floor of the eastern Tibetan plateau. *Environ. Sci. Technol.* 51, 801–809.

- Wang, X., Yuan, W., Lin, C.-J., Zhang, L., Zhang, H., Feng, X., 2019. Climate and vegetation as primary drivers for global mercury storage in surface soil. *Environ. Sci. Technol.* 53, 10665–10675.
- USEPA, 2002. Method 1631, Revision E: Mercury in Water by Oxidation, Purge and Trap, and Cold Vapor Atomic Fluorescence Spectrometry. US Environmental Protection Agency, Washington, DC.
- Wang, Z., Chen, J., Feng, X., Hintelmann, H., Yuan, S., Cai, H., et al., 2015. Mass-dependent and mass-independent fractionation of mercury isotopes in precipitation from Guiyang, SW China. *Comptes Rendus Geoscience* 347, 358–367.
- Wiesmeier, M., Spörlein, P., Geuß, U., Hangen, E., Haug, S., Reischl, A., et al., 2012. Soil organic carbon stocks in Southeast Germany (Bavaria) as affected by land use, soil type and sampling depth. *Glob. Chang. Biol.* 18, 2233–2245.
- Xue, W., Kwon, S.Y., Grasby, S.E., Sunderland, E.M., Pan, X., Sun, R., et al., 2019. Anthropogenic influences on mercury in Chinese soil and sediment revealed by relationships with total organic carbon. *Environ. Pollut.* 255, 113186.
- Yin, R., Feng, X., Meng, B., 2013a. Stable mercury isotope variation in rice plants (*Oryza sativa* L.) from the Wanshan mercury mining district, SW China. *Environ. Sci. Technol.* 47, 2238–2245.
- Yin, R., Feng, X., Wang, J., Bao, Z., Yu, B., Chen, J., 2013b. Mercury isotope variations between bioavailable mercury fractions and total mercury in mercury contaminated soil in Wanshan mercury mine, SW China. *Chemical geology* 336, 80–86.
- Yin, R., Feng, X., Chen, J., 2014. Mercury stable isotopic compositions in coals from major coal producing fields in China and their geochemical and environmental implications. *Environ. Sci. Technol.* 48, 5565–5574.
- Yin, R., Feng, X., Hurley, J.P., Krabbenhoft, D.P., Lepak, R.F., Hu, R., et al., 2016a. Mercury isotopes as proxies to identify sources and environmental impacts of mercury in sphalerites. *Sci. Rep.* 6, 1–8.
- Yin, R., Krabbenhoft, D.P., Bergquist, B.A., Zheng, W., Lepak, R.F., Hurley, J.P., 2016b. Effects of mercury and thallium concentrations on high precision determination of mercury isotopic composition by Neptune plus multiple collector inductively coupled plasma mass spectrometry. *J. Anal. At. Spectrom.* 31, 2060–2068.
- Yu, B., Yang, L., Liu, H., Xiao, C., Bu, D., Zhang, Q., et al., 2022. Tracing the transboundary transport of mercury to the Tibetan plateau using atmospheric mercury isotopes. *Environ. Sci. Technol.* 56, 1568–1577.
- Yuan, S., Zhang, Y., Chen, J., Kang, S., Zhang, J., Feng, X., et al., 2015. Large variation of mercury isotope composition during a single precipitation event at Lhasa City, Tibetan plateau, China. *Procedia Earth and Planetary Science* 13, 282–286.
- Zambardi, T., Sonke, J., Toutain, J., Sortino, F., Shinohara, H., 2009. Mercury emissions and stable isotopic compositions at Vulcano Island (Italy). *Earth Planet. Sci. Lett.* 277, 236–243.
- Zhang, H., Feng, X., Larssen, T., Qiu, G., Vogt, R.D., 2010. In inland China, rice, rather than fish, is the major pathway for methylmercury exposure. *Environ. Health Perspect.* 118, 1183–1188.
- Zhang, H., Yin, R.-s., Feng, X.-b., Sommar, J., Anderson, C.W., Sapkota, A., et al., 2013. Atmospheric mercury inputs in montane soils increase with elevation: evidence from mercury isotope signatures. *Sci. Rep.* 3, 1–8.
- Zheng, W., Obrist, D., Weis, D., Bergquist, B.A., 2016. Mercury isotope compositions across north American forests. *Global Biogeochem. Cycles* 30, 1475–1492.
- Zhu, W., Lin, C.-J., Wang, X., Sommar, J., Fu, X., Feng, X., 2016. Global observations and modeling of atmosphere–surface exchange of elemental mercury: a critical review. *Atmospheric Chemistry and Physics* 16, 4451–4480.